ACS APPLIED MATERIALS & INTERFACES

Research Article

www.acsami.org

Ionic Iridium Complex and Conjugated Polymer Used To Solution-Process a Bilayer White Light-Emitting Diode

Michele Sessolo, Daniel Tordera, and Henk J. Bolink*

Instituto de Ciencia Molecular, Universidad de Valencia, ES-46980 Paterna (Valencia), Spain

Supporting Information

ABSTRACT: Bilayer white light-emitting devices are prepared from solution, using an ionic orange phosphorescent organometallic complex and a neutral fluorescent conjugated polymer. Because of the very different polarity of the two components, they dissolve in orthogonal solvents, allowing for the direct deposition of the blue emitter on top of the orange emitter without the need of cross-linking or special coating methodology. Fine tuning of the layer thickness of both light-emitting layers allows for the color tuning of different types of white light.

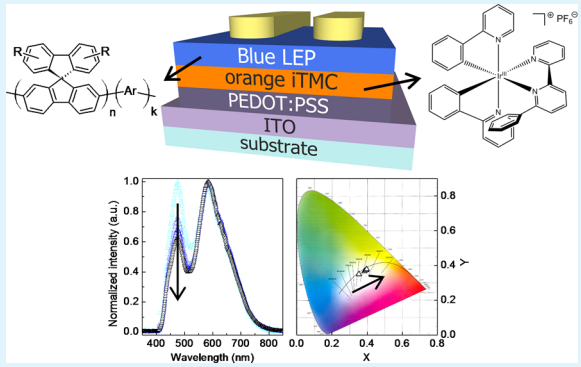

KEYWORDS: *multilayer, ionic transition metal complex, electroluminescence, light emitting polymer, solution process, white light*

INTRODUCTION

In the last two decades, organic light-emitting diodes (OLEDs) have been the subject of intense research that has brought them from basic laboratory research into the market of flat displays.[1,2] On the other hand, white OLEDs (WOLEDs) for lighting application are still far from experiencing a successful market entrance, and many issues have to be solved in order to make them a viable alternative to the current lighting technologies.[3] In particular, a strong reduction of the manufacturing costs must be addressed. Efficient commercial OLED displays consist of multilayer devices fabricated by subsequent deposition of functional organic molecules in high vacuum chambers, a technique which obviously limits the production throughput and inflates the final cost of the device. This makes efficient WOLEDs too expensive to be competitive in the lighting market.

Solution processing methods represents the most cost-efficient alternative in the deposition of organic materials, since it would allow preparing devices through established large area coating/printing techniques on virtually any type of substrate. Nevertheless, the preparation of multilayer structures by solution processing remains challenging. Since organic semiconductors have similar solubility in organic solvents, the subsequent deposition of thin layers on top of each other leads to intermixing and morphological damage of the organic films. Several strategies have been proposed to address this problem, typically consisting of making the bottom layer invulnerable to the deposition of the next one. A successful approach is the use of cross-linkable semiconducting polymers that can be made insoluble through simple photocuring or thermal curing.[4−8] These materials have the additional advantage of enabling direct patterning through conventional photolithography, which is desired to define OLED pixels in displays applications.[9,10] Besides the high versatility of this method, the addition of curing agents into the organic semiconductors leads to the presence of considerable amounts of chemical residues that might undermine the device stability. A similar approach is the use of high- and/or long-temperature annealing treatments in order to make an insoluble polymeric thin film.[11−16] However, the thickness and morphology of the annealed polymer layers are difficult to control, and most of the time, the subsequent deposition of a top layer causes partial dissolution or damage of the bottom layer. A more elegant approach is the use of orthogonal materials, which consists of the alternate deposition of hydrophobic and hydrophilic species from organic and polar solvents, respectively.[17] With this respect, conjugated polyelectrolytes have gained much attention as charge transport materials, while, more recently, it has been demonstrated how fluorinated polymers simultaneously enables both orthogonal processing and direct patterning through photolithography.[18−20]

All the mentioned techniques rely on sophisticated chemical modifications of the organic semiconductors in order to obtain multilayer structures with neat interfaces and reproducible electronic behavior. In this communication, we demonstrate solution processed multilayered white OLEDs employing a standard conjugated polymer combined with ionic transition-metal complexes (iTMCs). The latter class of compounds is

Received: September 18, 2012
Accepted: January 17, 2013
Published: January 17, 2013

characterized by high photoluminescence quantum yields (nearly quantitative in solid state), tunable emission over the entire spectral range, and quantitative yield synthesis.[21−23] With these motivations, iTMCs have been successfully employed in light-emitting electrochemical cells (LECs), as a simpler alternative to standard OLEDs.[24−27] Their poor solubility in organic solvents and their high solubility in polar solvents make them ideal candidates in the preparation of multilayered, solution-processed light-emitting devices. As a proof of principle, we demonstrate that simple solution processed multilayered WOLEDs can be prepared by combining a thin layer of an orange light-emitting iTMC with a film of a blue-emitting polymer. By tuning the iTMC and polymer film thickness, bright white electroluminescence with variable color temperature can be obtained, demonstrating the versatility and potential of this approach.

EXPERIMENTAL SECTION

Aqueous dispersions of poly(3,4-ethylenedioxythiophene) doped with poly(styrenesulfonate) (PEDOT:PSS, CLEVIOS P VP Al 4083) were obtained from Heraeus Holding GmbH and used as received. The ionic transition-metal complex (iTMC) 6-phenyl-2,2′-bipyridine (bis[2-(phenyl)pyridinato]iridium(III) hexafluorophosphate [Ir(ppy)$_2$(Hpbpy)][PF$_6$] was synthesized following a previously published procedure.[28] The ionic liquid (IL) 1-butyl-3-methyl imidazolium hexafluorophosphate (BMImPF$_6$) was purchased from Aldrich. The blue-emitting polymer CB02 was obtained from Merck OLED Materials GmbH.

Commercial patterned indium tin oxide (ITO)-coated glass substrates (www.naranjosubstrates.com) were thoroughly cleaned through chemical and UV-ozone methods and used as the transparent anodes. Sixty nanometer thick PEDOT:PSS layers were spin-coated on top of the conductive substrates and subsequently annealed at 150 °C for 30 min. Thin films of [Ir(ppy)$_2$(Hpbpy)](PF$_6$) with variable thickness were spin-coated on top of the PEDOT:PSS from acetonitrile by varying the concentration of the solutions (typically from 0.25 wt % to 0.5 wt %). Small amounts of IL were added to the metal complex solution in order to enhance the ionic conductivity of the resulting layers.[29] After spin coating, films were dried in an ambient atmosphere at 150 °C for 5 min. The blue-emitting layers were deposited on top of the iTMC films by spin-coating of mesitylene solutions of the CB02. All solutions were filtered over a 0.20-μm polytetrafluoroethylene filter before the deposition. Finally, the metal cathodes composed by Ba (5 nm) and Ag (100 nm) were evaporated in a high vacuum chamber integrated in an inert glovebox atmosphere under a base pressure of 1×10^{-6} mbar.

All device measurements were performed in an inert atmosphere. Thicknesses of the organic films were determined using an Ambios XP1 profilometer (limit ∼1 nm). The current-density-versus-voltage (J−V) and electroluminescence-versus-voltage (L−V) characteristics were collected using a Keithley Model 2400 source measurement unit and a Si-photodiode coupled to a Keithley Model 6485 picoamperometer, respectively. The photocurrent was calibrated using a Minolta Model LS100 luminance meter. Electroluminescence spectra were recorded using an Avantis fiber-optics photospectrometer.

RESULTS AND DISCUSSION

In the device architecture presented here (Figure 1), it is essential that the solution processing of the top blue-emitting polymer does not cause dissolution or damage of the underlying active film. This can be achieved by using mesitylene as the solvents for the CB02 deposition, which has a dielectric constant of ∼2.3.[30] The extremely low polarity of mesitylene ensures that no etching of the hydrophilic iTMC layer occurs during the polymer processing, resulting in a neat and homogeneous heterojunction between the two materials. This

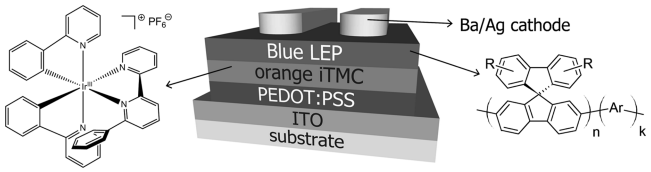

Figure 1. Schematic view of the multilayered white organic light-emitting diodes (OLEDs) with the chemical structure of the active species used as emitters.

was verified by analyzing the ultraviolet−visible light (UV-vis) absorption spectra of the iTMC film upon sequential rinsing with mesitylene (see Figure S1 in the Supporting Information). No changes were observed in the absorption spectra. Since the absorption spectra are very sensitive to variations in film thickness, this implies that no redisolving of the iTMC layer occurs in this process. In addition to this, atomic force microscopy (AFM) images were obtained from the pristine and mesitylene-rinsed iTMC layers (Figure 2). The films appear very smooth before and after rinsing with mesitylene, which again indicates that the iTMC film is not affected by coating a second film from a mesitylene solution on top of it.

Various devices with different layer thicknesses of both the iTMC and the polymer layer have been tested, in order to find a balance in the emission of the respective materials. Here, we present a series of three devices, where the thickness of the blue-emitting polymer layer is kept constant at 70 nm, while the thickness of the iTMC is tuned from 20 nm (dev. X) to 25 nm (dev. Y) and 30 nm (dev. Z). We will show how such a small dimensional difference has a drastic effect on the emission spectra of the bilayer devices.

In Figure 3, the current density and luminance versus voltage (JVL) characteristics of the three devices are reported. The current density (Figure 3a) flowing through the three devices is similar, because of the small difference in the iTMC layer thickness. Interestingly, current starts to be injected at a voltage (∼5 V) that is much higher, compared to the difference in energy between the two electrodes (∼2.4 eV, −5.1 eV and −2.7 eV from the vacuum level for ITO/PEDOT:PSS and Ba, respectively). Since the CB02/Ba contact is ohmic, this effect is likely due to the presence of a relatively high energy barrier at the PEDOT:PSS/iTMC interface or to the ions redistribution in the ionic layer under the applied field (Figure 3a).[31−33] Light emission (Figure 3b) turns on at approximately the same voltage, increasing till values comprises between 200 and 700 cd/m^2 are reached at 10 V, for devices X-Y and Z, respectively. The resulting efficacy increase as the iTMC layer thickness is increased, from 0.41 cd/A for device X, 0.46 cd/A for device Y, and 0.90 cd/A for device Z (see inset of Figure 3b). This trend is not unexpected, since the orange emitter itself can lead to much more efficient devices, compared to the blue polymer, and a thicker layer should enhance the orange emission, as discussed later in this work.[28,34] The low efficacy of these WOLEDs, compared to, for example, the single-layer devices employing CB02 or [Ir(ppy)$_2$(Hpbpy)](PF$_6$) as active materials, is probably due to exciton quenching phenomena. Single-layer devices using CB02 were published previously by our group and showed slightly lower current densities at similar driving voltages.[35] However, in these single-layer CB02 devices, the current efficiency was higher, reaching values of 2 cd/A when PEDOT:PSS was used as the hole injection layer. A direct comparison with a single-layer device using [Ir(ppy)$_2$(Hpbpy)](PF$_6$) as the active material as described in

dx.doi.org/10.1021/am302033k | ACS Appl. Mater. Interfaces 2013, 5, 630−634

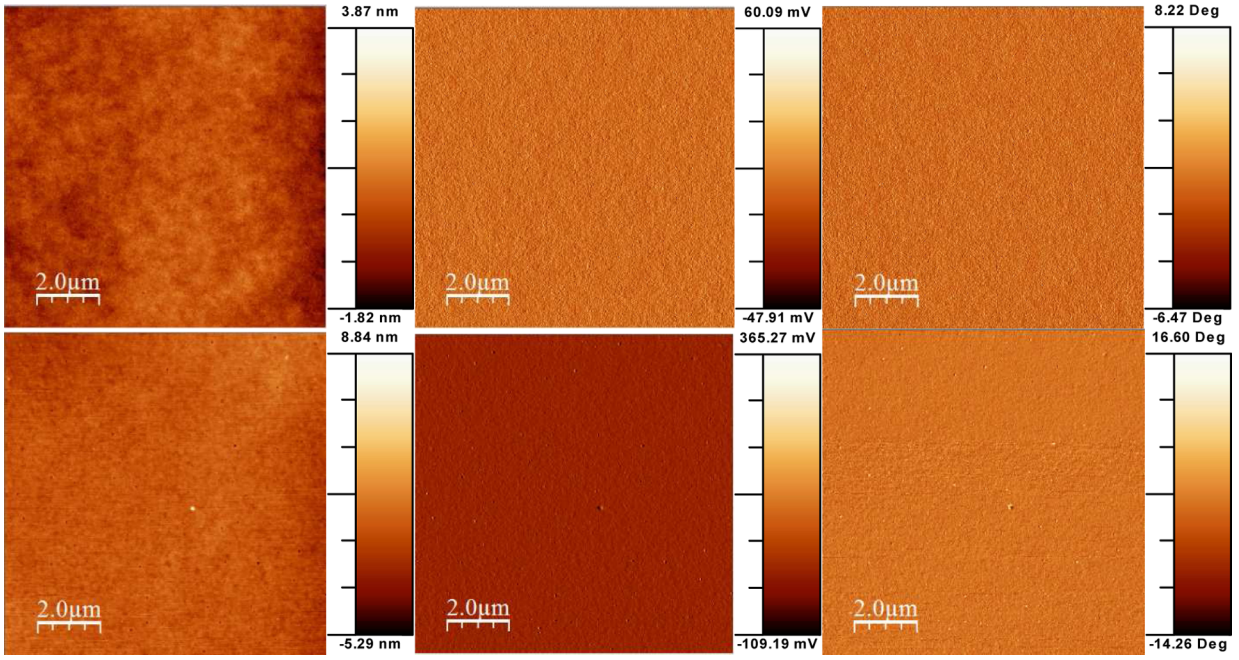

Figure 2. Atomic force microscopy (AFM) images of an ionic transition-metal complex (iTMC) layer (top row) and iTMC layer rinsed with mesitylene (bottom row), depicting height, amplitude, and phase. Measurements were performed on a 10 μm × 10 μm surface.

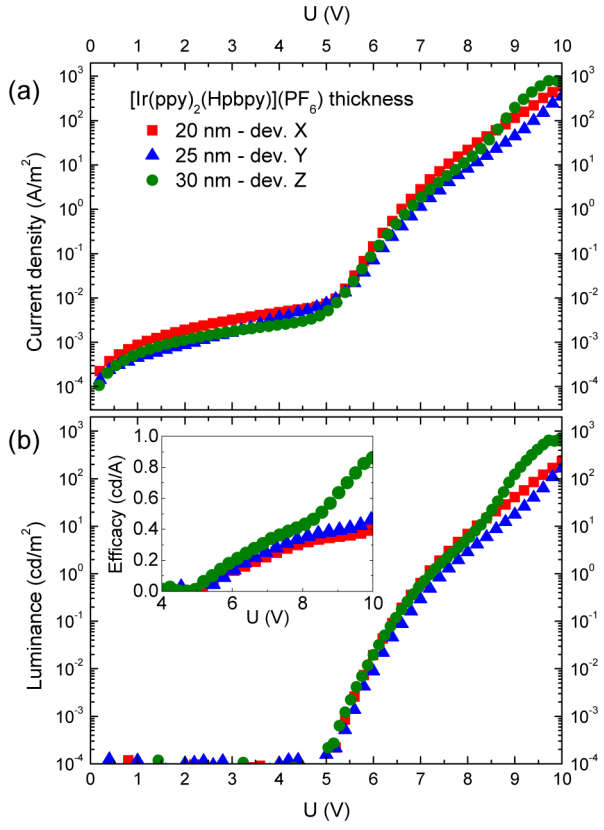

Figure 3. Current density (a) and luminance (b) versus applied bias for a series of bilayer OLEDs with structure ITO/PEDOT:PSS (60 nm)/iTMC (x nm)/CB02 (70 nm)/Ba (5 nm)/Ag (100 nm), with increasing thickness of the $[Ir(ppy)_2(Hpbpy)](PF_6)$ orange iTMC emitter. Inset of Figure 3a shows the efficacy versus the applied bias for the same devices.

ref 28 is not so straightforward. In such a device, the charge injection is dependent on the movement of ions toward the respective electrodes, leading to the formation of dynamically doped layers. Therefore, the current density and luminance versus voltage analysis are time-dependent. In our double-layer devices, the formation of doped zones is not occurring, because of the ion-free top CB02 layer. Because of this, no increase of the $J-V$ curves is observed with increasing operation time. Nevertheless, below the potential origin of the low efficiencies observed in this particular bilayer devices is commented upon.

In a first approximation, the exciton generation zone can extend over both the orange- and blue-emitting layers, since only a low energy barrier is present at the heterojunction for both negative and positive carriers (Figure 4a). The singlet excitons generated in the polymer can either radiatively recombine or migrate to the heterojunction where they are transferred to the iTMC. The same is true for the nonemissive polymer triplet exciton, which, in principle, can migrate in the orange layers and thus potentially contribute to the overall electroluminescence. Unfortunately, the triplet energy of the phosphorescent and fluorescent materials are similar (Figure 4b), and the back transfer of excitons from the iTMC layer to the polymer can also occur. This possibility is valid also for the triplet excitons directly generated in the iTMC. These processes would mean that a large number of potentially emissive states are lost due to the energy transfer to nonemissive triplet states in the polymer. Finally, exciton separation cannot be excluded at both the PEDOT:PSS/iTMC or the CB02/Ba interfaces.

The electroluminescence spectra for the bilayer WOLEDs, as a function of the $[Ir(ppy)_2(Hpbpy)](PF_6)$ layer thickness as well as the applied bias, are reported in Figure 5. The corresponding colors, expressed as Commission Internationale de L'Eclairage (CIE) coordinates, are also included.

The spectra of device X (20 nm iTMC layer thickness) at 6 V shows a broad emission that extends over the entire visible range, with an intense peak centered at 475 nm and a weaker shoulder at ~580 nm, which is characteristic of the blue and orange emission of the CB02 and $[Ir(ppy)_2(Hpbpy)](PF_6)$,

dx.doi.org/10.1021/am302033k | ACS Appl. Mater. Interfaces 2013, 5, 630−634

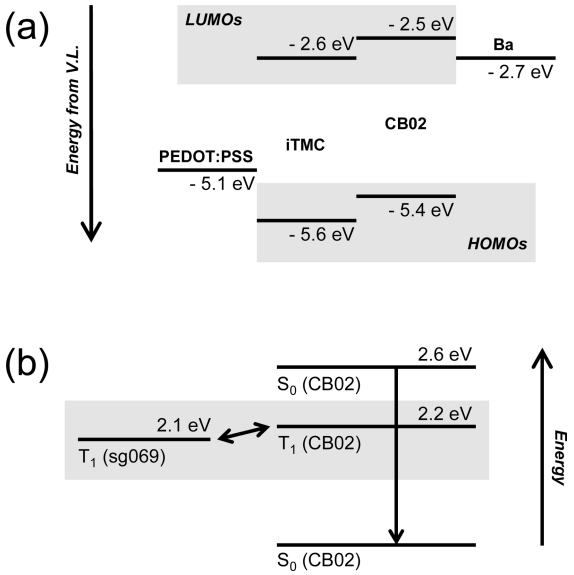

Figure 4. (a) Scheme of the energy levels of the materials employed in the devices. (b) Schematic representation of the energy levels with different spin multiplicity involved in the electroluminescence. Energy levels are taken from literature data.[28,34,36,37]

respectively. The correspondent color point lies at the frontier between the white zone and the blue zone of the CIE diagram, because of the dominant CB02 emission. Increasing applied bias (7 V) lead to an enhancement of the orange emission with a consequent shift of the color coordinates very close to the white point (x = 0.324, y = 0.337; white point: $x = y = {}^{1}/_{3}$). This demonstrates how, with this simple double layer structure, an almost-ideal white emission can be obtained. Higher applied biases further increase the orange emission of the iTMC (Figure 5a), with only a small shift in the correspondent color points that keep being centered in the white zone and aligned to the blackbody emission curve. The fact that the blue emission is dominant at low bias suggests that the recombination zone should be located at the heterojunction but extends into the polymer layer. The evolution of the spectra can be attributed to a narrowing of the emission zone in the vicinity of the iTMC/CB02 heterojunction at higher driving voltage. Figure 5b reports the electroluminescence spectra for the device with a 25-nm-thick $[Ir(ppy)_2(Hpbpy)](PF_6)$ film (device Y). At low bias (7 V), the blue and orange components have similar intensity, leading to color coordinates that are, again, very close to the white point (x = 0.353, y = 0.350). The electroluminescence spectra evolve with increasing voltages, as observed for device Y, with an augmented intensity of the iTMC orange emission to the detriment of the blue component. In this case, however, the spectra and the correspondent color coordinate variations are greatly reduced in the 8−10 V bias range, showing a stable and white electroluminescence. Further increases in the iTMC layer thickness (30 nm, device Z) lead to an almost-voltage-independent emission spectra profile (see Figure 5c), characterized by a weak blue emission and a very strong orange phosphorescence, which causes the correspondent color coordinates to settle at the edge between the white zone and the orange zone of the CIE diagram.

In addition to being a demonstration of the possibility of preparing a simple solution-processed bilayer WOLED, the electroluminescence data give important insights of the optoelectronic processes that are occurring within the device itself. The emission zone is likely to be located close to the iTMC/CB02 heterojunction, since emission from both materials was measured independently on the applied bias and iTMC layer thickness. At low driving voltage, for a thin orange-emitting layer (dev. X), the blue emission is 2 times stronger than the orange one, meaning that the recombination

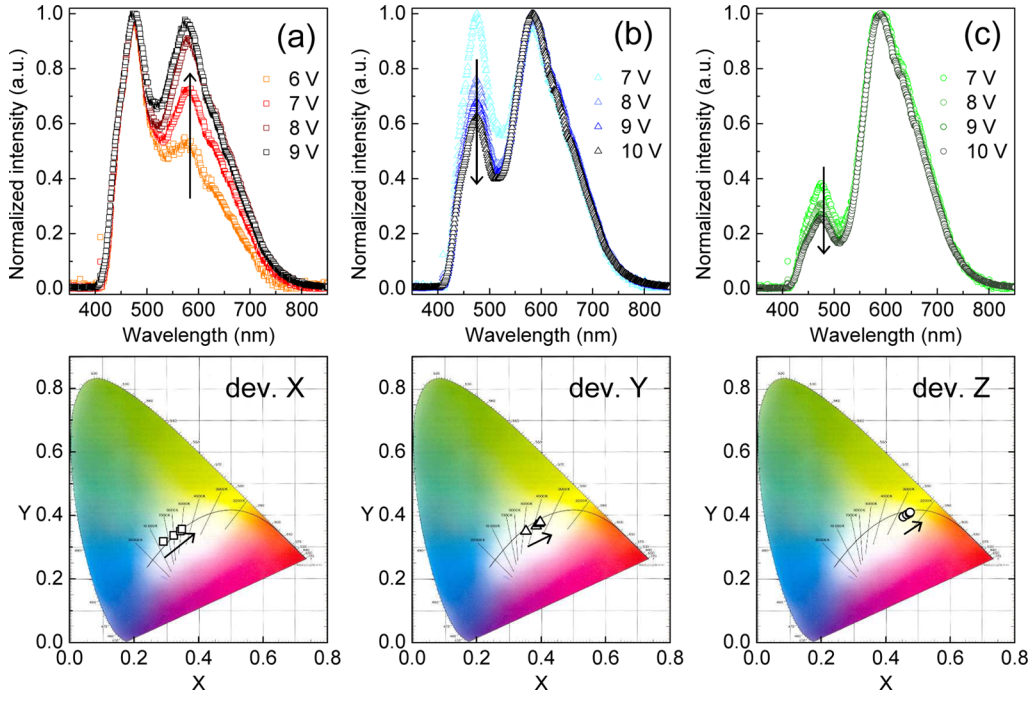

Figure 5. Normalized electroluminescence spectra for device X (a), Y (b), and Z (c), recorded at increasing driving voltage. The bottom graphs report the correspondent CIE color coordinates (bottom). The black arrows indicate increasing driving voltages.

dx.doi.org/10.1021/am302033k | ACS Appl. Mater. Interfaces 2013, 5, 630−634

zone extends into the CB02 film. Increasing the bias augments the electron density in the device, inducing a shift of the recombination zone toward the iTMC layer. The same effect can be obtained by changing the $[Ir(ppy)_2(Hpbpy)](PF_6)$ layer thickness, resulting in a strong orange electroluminescence, even at low bias, as observed for devices Y and Z. This means that the color of the emission in this solution-processed OLED can be finely tuned through the control of the layer thicknesses and driving voltage.

CONCLUSIONS

A novel solution-processed multilayer white organic light-emitting diode (WOLED) architecture that combines materials dissolving in orthogonal solvents has been presented. The use of an ionic organometallic complex allows for the preparation of a multilayer architecture by simple solution processing, thanks to their unique solubility in polar solvents. Through an accurate tuning of the layer thickness of the emissive materials, white emission with color coordinates close to the Commission Internationale de L'Eclairage (CIE) white point were obtained.

ASSOCIATED CONTENT

Supporting Information

UV-vis absorption spectra can be found in the Supporting Information. This information is available free of charge via the Internet at http://pubs.acs.org/.

AUTHOR INFORMATION

Corresponding Author

*E-mail: henk.bolink@uv.es.

Notes

The authors declare no competing financial interest.

ACKNOWLEDGMENTS

We are grateful to Edwin Constable and Gabriel Schneider (University of Basel), for supply of the iridium complex. This work has been supported by the Spanish Ministry of Economy and Competitiveness (MINECO) (No. MAT2011-24594). D.T. acknowledges the Spanish Ministry of Education, Culture, and Sport for an FPU grant.

REFERENCES

(1) Tang, C. W.; Vanslyke, S. A. *Appl. Phys. Lett.* **1987**, *51*, 913.
(2) Semenza, P. *Inf. Disp.* **2010**, *26*, 14−17.
(3) Gather, M. C.; Köhnen, A.; Meerholz, K. *Adv. Mater.* **2011**, *23*, 233−248.
(4) Chen, J. P.; Klaerner, G.; Lee, J.-I.; Markiewicz, D.; Lee, V. Y.; Miller, R. D.; Scott, J. C. *Synth. Met.* **1999**, *107*, 129−135.
(5) Zhang, Y.-D.; Hreha, R. D.; Jabbour, G. E.; Kippelen, B.; Peyghambarian, N.; Marder, S. R. *J. Mater. Chem.* **2002**, *12*, 1703−1708.
(6) Huang, F.; Cheng, Y.-J.; Zhang, Y.; Liu, M. S.; Jen, A. K.-Y. *J. Mater. Chem.* **2008**, *18*, 4495−4498.
(7) Köhnen, A.; Riegel, N.; Kremer, J. H.-W. M.; Lademann, H.; Müller, D. C.; Meerholz, K. *Adv. Mater.* **2010**, *21*, 879−884.
(8) Png, R.; Chia, P.; Tang, J.; Liu, B.; Sivaramakrishnan, S.; Zhou, M.; Khong, S.; Chan, H. S. O.; Burroughes, J. H.; Chua, L. L.; Friend, R. H.; Ho, P. K. H. *Nat. Mater.* **2010**, *9*, 152−158.
(9) Muller, C. D.; Falcou, A.; Reckefuss, N.; Rojahn, M.; Wiederhirn, V.; Rudati, P.; Frohne, H.; Nuyken, O.; Becker, H.; Meerholz, K. *Nature* **2003**, *421*, 829−833.
(10) Gather, M. C.; Köhnen, A.; Falcou, A.; Becker, H.; Meerholz, K. *Adv. Funct. Mater.* **2007**, *17*, 191−200.
(11) Gong, X.; Moses, D.; Heeger, A. J.; Liu, S.; Jen, A. K.-Y. *Appl. Phys. Lett.* **2003**, *83*, 183.
(12) Yan, H.; Scott, B. J.; Huang, Q.; Marks, T. J. *Adv. Mater.* **2004**, *16*, 1948−1953.
(13) Ho, G.-K.; Meng, H.-F.; Lin, S.-C.; Horng, S.-F.; Hsu, C.-S.; Chen, L.-C.; Chang, S.-M. *Appl. Phys. Lett.* **2004**, *85*, 4576.
(14) Kim, J.-S.; Friend, R. H.; Grizzi, I.; Burroughes, J. H. *Appl. Phys. Lett.* **2005**, *87*, 023506.
(15) Yang, X. H.; Jaiser, F.; Stiller, B.; Neher, D.; Galbrecht, F.; Scherf, U. *Adv. Funct. Mater.* **2006**, *16*, 2156−2162.
(16) Köhnen, A.; Irion, M.; Gather, M. C.; Rehmann, N.; Zacharias, P.; Meerholz, K. *J. Mater. Chem.* **2010**, *20*, 3301−3306.
(17) Gong, X.; Wang, S.; Moses, D.; Bazan, G. C.; Heeger, A. J. *Adv. Mater.* **2005**, *17*, 2053−2058.
(18) Wu, H.; Huang, F.; Mo, Y.; Yang, W.; Wang, D.; Peng, J.; Cao, Y. *Adv. Mater.* **2004**, *16*, 1826−1830.
(19) Duarte, A.; Pu, K.-Y.; Liu, B.; Bazan, G. C. *Chem. Mater.* **2011**, *23*, 501−515.
(20) Fong, H. H.; Lee, J.-K.; Lim, Y.-F.; Zakhidov, A. A.; Wong, W. W. H.; Holmes, A. B.; Ober, C. K.; Malliaras, G. G. *Adv. Mater.* **2011**, *23*, 735−739.
(21) Bolink, H. J.; Coronado, E.; Costa, R. D.; Lardiés, N.; Ortí, E. *Inorg. Chem.* **2008**, *47*, 9149−9151.
(22) Tamayo, A. B.; Garon, S.; Sajoto, T.; Djurovich, P. I.; Tsyba, I.; Bau, R.; Thompson, M. E. *Inorg. Chem.* **2005**, *44*, 8723−8732.
(23) Sprouse, S.; King, K. A.; Spellane, P. J.; Watts, R. J. *J. Am. Chem. Soc.* **1984**, *106*, 6647−6653.
(24) Buda, M.; Kalyuzhny, G.; Bard, A. J. *J. Am. Chem. Soc.* **2002**, *124*, 6090−6098.
(25) Slinker, J.; Bernards, D.; Houston, P. L.; Abruña, H. D.; Bernhard, S.; Malliaras, G. G. *Chem. Commun.* **2003**, 2392−2399.
(26) Bolink, H. J.; Cappelli, L.; Coronado, E.; Graetzel, M.; Nazeeruddin, M. *J. Am. Chem. Soc.* **2006**, *128*, 46−47.
(27) Slinker, J.; Rivnay, J.; Moskowitz, J. S.; Parker, J. B.; Bernhard, S.; Abruña, H. D.; Malliaras, G. G. *J. Mater. Chem.* **2007**, *17*, 2976−2988.
(28) Bolink, H. J.; Coronado, E.; Costa, R. D.; Ortí, E.; Sessolo, M.; Graber, S.; Doyle, K.; Neuburger, M.; Housecroft, C. E.; Constable, E. C. *Adv. Mater.* **2008**, *20*, 3910−3913.
(29) Parker, S. T.; Slinker, J. D.; Lowry, M. S.; Cox, M. P.; Bernhard, S.; Malliaras, G. G. *Chem. Mater.* **2005**, *17*, 3187−3190.
(30) Kwak, K.; Park, S.; Fayer, M. D. *Proc. Natl. Acad. Sci. U.S.A.* **2007**, *104*, 14221−14226.
(31) Slinker, J. D.; DeFranco, J. A.; Jaquith, M. J.; Silveira, W. R.; Zhong, Y.-W.; Moran-Mirabal, J. M.; Caraighead, H. G.; Abruña, H. D.; Marohn, J. A.; Malliaras, G. G. *Nat. Mater.* **2007**, *6*, 894−899.
(32) Van Reenen, S.; Matbya, P.; Dzwilwsky, A.; Janssen, R. A. J.; Edman, L.; Kemerink, M. *J. Am. Chem. Soc.* **2010**, *132*, 13776−13781.
(33) Lenes, M.; Garcia-Belmonte, G.; Tordera, D.; Pertegás, A.; Bisquert, J.; Bolink, H. J. *Adv. Funct. Mater.* **2011**, *21*, 1581−1586.
(34) Suh, M. C.; Chin, B. D.; Kim, M.-H.; Kang, T. M.; Lee, S. T. *Adv. Mater.* **2003**, *15*, 1254−1258.
(35) Bolink, H. J.; Coronado, E.; Forment-Aliaga, A.; Gómez-Gacía, C. J. *Adv. Mater.* **2005**, *17*, 1018−1023.
(36) D'Andrade, B. W.; Datta, S.; Forrest, S. R.; Djurovich, P.; Polikarpov, E.; Thompson, M. E. *Org. Electron.* **2005**, *6*, 11−20.
(37) Djurovich, P.; Mayo, E. I.; Forrest, S. R.; Thompson, M. E. *Org. Electron.* **2009**, *10*, 515−520.